Electric Field-Enhanced Generation Current in Proton Irradiated InGaAs Photodiodes

Marco Benfante, Jean-Luc Reverchon, Olivier Gilard, Stéphane Demiguel, Cédric Virmontois, Clémentine Durnez, Thierry Dartois, Vincent Goiffon

Electric Field Enhanced Generation Current in Proton Irradiated InGaAs Photodiodes

M. Benfante, J-L. Reverchon, O. Gilard, S. Demiguel, C. Virmontois, C. Durnez, T. Dartois, and V. Goiffon

***Abstract*—Dark current degradation due to 49.7 MeV proton irradiation is studied on lattice-matched InGaAs PIN photodiodes. This degradation is described in terms of electric field enhanced Shockley-Read-Hall generation current in the depletion region. In this paper we present a model of the radiation-induced generation current which includes the role of the electric field through the generation rate field enhancement factor (GRFEF). Using a combination of dark current-voltage and capacitance-voltage measurements, an experimental GRFEF is extracted for the thermal generation rate. This GRFEF has been used to define a new damage factor for InGaAs at low electric field that has been compared to previous literature studies. As a final result, the low-field generation lifetime degradation as a function of the fluence has been extracted.**

***Index Terms*—Damage factor, dark current, electric field enhancement, indium gallium arsenide (InGaAs), photodiodes, proton irradiation, Shockley-Read-Hall, generation lifetime.**

I. Introduction

THE effects of space radiation on indium gallium arsenide (InGaAs) photodiodes have been an object of attention of physicists and engineers for the last 25 years [1]. InGaAs, with a gap at 300 K of 0.74 eV (corresponding to a cutoff wavelength of $\lambda_c \approx 1.67$ µm) is a suitable semiconductor in the Short Wavelength InfraRed (SWIR) domain. Examples of space applications for such devices are earth observation (vegetation, ice) and satellite-to-satellite or satellite-to-ground telecommunications. Such missions require a low dark current at high operating temperature ($\approx$ 250 K). InGaAs has shown promise as a good candidate to replace MCT (Mercury Cadmium Telluride or HgCdTe) for high temperature operation. Several studies have been done on the effects of proton irradiation on the dark current of InGaAs photodiodes [2]–[6]. Barde et al. [5] showed that dark current spikes and Random Telegraph Signals (RTS) observed in the frame of SPOT4 (Satellite pour l'Observation de la Terre 4) mission on lattice-matched InGaAs ($In_{0.53}Ga_{0.47}As$) detector modules can be explained by the effects of proton irradiation. Moreover, they affirmed that this degradation was due to the degradation of InGaAs itself, and not to the degradation of the Charge Coupled Device (CCD) readout circuit. Tauziede et al. [2] studied the effects of proton irradiation on InGaAs pixel arrays called "Cactus" produced at III-V Lab, France. The Read Out Integrated Circuit (ROIC) consisted of a Capacitance TransImpedance Amplifier (CTIA) circuit. They noticed an increase of the peak dark current and average dark current after irradiation, with a higher increase for low proton energies. Moreover, they found an increase of RTS amplitude with integration time and temperature. Kleipool et al. [6] analyzed the degradation of InGaAs pixel arrays that had been aboard the SCIAMACHY (SCanning Imaging Absorption spectroMeter for Atmospheric CHartographY) instrument of ENVISAT (Environmental SAtellite). The module's channel consisting of $In_{0.53}Ga_{0.47}As$ did not show any degradation, contrary to what has been seen in [5]. The authors tried to justify these results by stating differences in the device properties and operation conditions. All the cited studies attribute degradation to displacement damage. Displacement damage is due to the displacement of the atoms from their lattice site caused by the interaction between the protons and the nuclei of the semiconductor atoms. This damage is responsible for the formation of extra electronic levels in the band gap which enhance the Shockley-Read-Hall (SRH) generation current in the depletion regions [7], [8].

In this paper, planar disk-shaped lattice-matched InGaAs photodiodes of different diameters are analyzed when irradiated with 49.7 MeV protons. The effects of proton irradiation are evaluated by means of the dark current degradation ΔJ combining dark current-voltage (I_d-V) and capacitance-voltage (C-V) measurements. We show that the dark current is strongly affected by the electric field in the depletion region of the diode. This is confirmed by an estimation of the activation energy extracted from the dark current characteristics. The effects of electric field enhancement on dark current [9] have been studied for pn junctions in other materials like Silicon [10], [11] or Germanium [12]. To the best of our knowledge, there are no previous studies of electric field enhancement effects on irradiated InGaAs photodiodes.

II. Experimental details

A cross section of an irradiated photodiodes is shown in Fig. 1. The pn junction is created by Zn diffusion. The high Zn concentration ($> 10^{18}$ cm^{-3}) makes the p-side degenerate. Therefore, the device can be considered as a one-sided pn junction. The epitaxial growth and process are typical of that used to fabricate InGaAs-based photodiodes [2], [3].

The proton irradiation has been carried out at Université Catholique de Louvain (UCL) in Louvain-La-Neuve, Belgium.

M. Benfante is with III-V Lab, ISAE-SUPAERO, CNES, Thales Alenia Space (e-mail: marco.benfante@3-5lab.fr, telephone: 0169415522).

J-L Reverchon is with III-V Lab, 1 Avenue Augustin Fresnel, 91767 Palaiseau, France (e-mail:jean-luc.reverchon@3-5lab.fr)

O. Gilard, C. Durnez and C. Virmontois are with the French Space Agency CNES, 31401 Toulouse Cedex 4, France (e-mail: olivier.gilard@cnes.fr; clementine.durnez@cnes.fr; cedric.virmontois@cnes.fr).

V. Goiffon is with ISAE SUPAERO, Université de Toulouse, 10 avenue E. Belin, F-31055, Toulouse, France (e-mail: vincent.goiffon@isae-supaero.fr).

S. Demiguel and T. Dartois are with Thales Alenia Space, 06156 Cannes La Bocca, France.

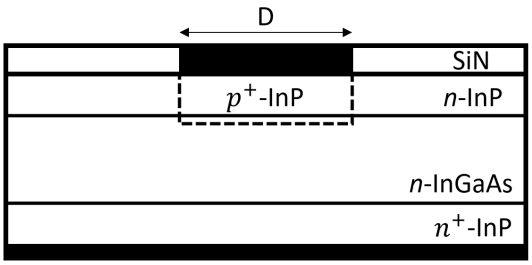

Fig. 1. Cross section of an InGaAs PIN photodiode. The black rectangles represent the two contacts. D is the diameter of the disk-shaped diode. The total thickness of the structure is 4 µm and the thickness of the InGaAs active layer is 3 µm.

TABLE I
PROTON IRRADIATION STEPS (E=49.7 MEV, T=293 K)

Step	**Cumulated fluence (cm^{-2})**	**Mean flux ($cm^{-2}s^{-1}$)**
1	1×10^{10}	2.16×10^{7}
2	3×10^{10}	3.96×10^{7}
3	1×10^{11}	1.11×10^{8}
4	3×10^{11}	1.49×10^{8}

This consisted of four steps described in Table I. The exposure was carried out at ambient temperature and the diode pins were short-circuited. The energy and fluences chosen corresponded to the typical doses received for the envisaged space missions. In the example of the SPOT4 mission, the expected Displacement Damage Dose received in a 7 years mission is approximately 4.5×10^7 MeV/g which corresponds to an equivalent 49.7 MeV proton fluence of about 1.5×10^{10} cm^{-2}.

$I_d - V$ measurements have been conducted at ambient temperature on the irradiation site before and after each fluence to study the dependence of the dark current on the fluence. $I_d - V$ and $C - V$ measurements were performed at the III-V Lab about one month after irradiation. In particular, temperature dependence of the $I_d - V$ has been studied between 270 K and 315 K in order to observe changes in the dark current activation energy of irradiated devices. The $C - V$ measurements have been performed at room temperature. Table II shows the different diameters of the disk-shaped diodes which have been analyzed to evaluate the impact of the dimensions on the dark current and to extract the diode capacitance.

III. MEASUREMENTS AND RESULTS

$I_d - V$ curves have been taken from -8 V to 0.4 V. Since InGaAs photodiodes are reverse biased during normal operation in real applications, only the reverse bias is considered.

TABLE II
DIODE LABELLING

Label	Diode1	Diode2	Diode3	Diode4	Diode5
Diameter (µm)	100	150	200	250	300

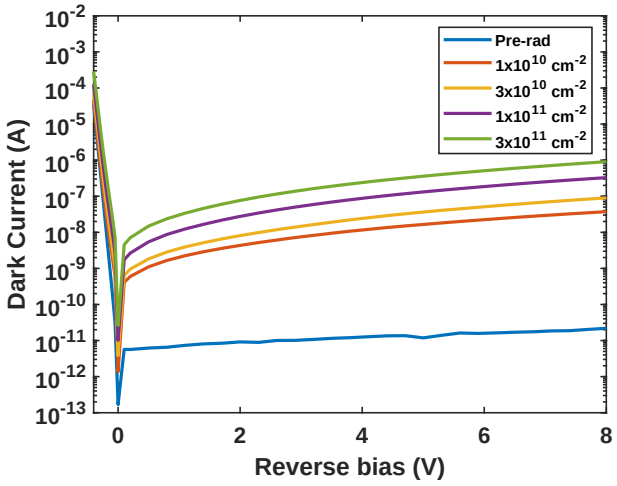

Fig. 2. Dark current evolution with fluence for Diode5. The dark current before irradiation is also drawn.

We limited the range to a maximum reverse bias of 8 V to avoid any band to band tunnel contribution. Figure 2 shows the dark current for Diode5 for all fluences. All the five diodes showed similar behavior.

Before irradiation, the contributions to the current from the perimeter and the area of the diode are comparable for the diameters considered. In particular, we found that the surface contribution is mainly a diffusion current whereas the perimeter contribution is a mix of diffusion current and SRH generation current. The same results were found by [13] who analyzed the dark current dependence on the size and temperature for the same photodiode structure as the one in the present paper. The temperature dependence of the dark current before irradiation shown in Fig. 3 proves the co-existence of these two contributions. At low bias, the generation current is negligible and the activation energy is the one of the InGaAs band gap energy whereas at larger bias the SRH current contribution makes the activation energy decrease. This is consistent with previous measurements on similar InGaAs photodiodes [14].

The effect of the proton irradiation on the photodiodes is to increase the dark current and to change its voltage dependence compared to pre-irradiation. In order to give an idea of the degradation rate, at 5 V, the dark current value on the pre-irradiated Diode5 is 1.19×10^{-11} A and it increases to 1.65×10^{-8} A at a fluence of 1×10^{10} cm^{-2}. Another effect of the proton irradiation is to make the dark current proportional to the surface. Figure 4 shows the dark current as a function of the diode area before irradiation as well as at the second and the fourth fluences.

A. Dark Current Dependence on Fluence

The dark current density degradation is defined as $\Delta J(\Phi) = J_{post}(\Phi) - J_{pre}$, where $J_{post}(\Phi)$ is the dark current density after irradiation at fluence Φ and J_{pre} is the dark current density before irradiation. It has been calculated by normalizing the dark current to the area given by the Zn

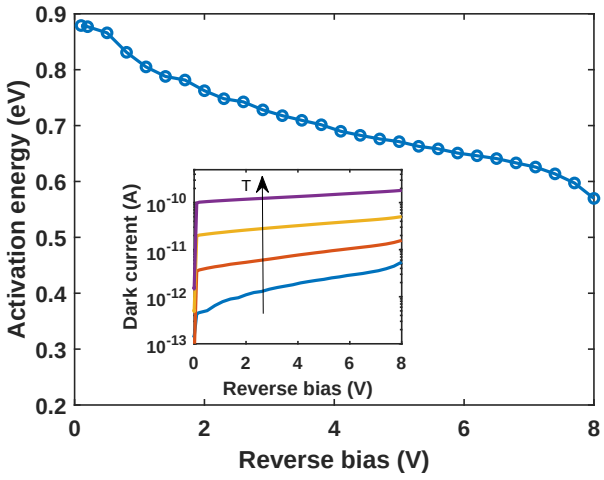

Fig. 3. Activation energy before irradiation. Inset: $I_d - V$ curve for temperatures: 270 K, 285 K, 300 K, 315 K.

diffusion. Figure 5 shows that the degradation is linear with fluence. All diodes showed this same dependence.

In order to contextualize these results, we comment on the role of the dark current in real space applications. The impact of dark current on detector performances is to decrease the Signal to Noise Ratio (SNR). Considering just the photoactive material we have:

$$\mathrm{SNR} = \frac{\mathrm{Signal}}{\mathrm{Noise}} = \gamma \frac{I_\mathrm{p}}{P_\mathrm{shot} + P_\mathrm{thermal}} \tag{1}$$

where $P_\mathrm{shot} = 2q(I_\mathrm{d} + I_\mathrm{p} + I_\mathrm{b})B$ is the shot noise, $P_\mathrm{thermal} = \frac{4kTB}{R}$ is the thermal noise [15] and γ is a proportionality coefficient. In these equations, q is the elementary charge, I_d is the dark current, I_p is the photocurrent due to the signal, I_b is the photocurrent due to the background, k is the Boltzmann constant, T is the temperature, B is the noise bandwidth and $R = \frac{\mathrm{d}I_d}{\mathrm{d}V}$ is the diode resistance. In imaging applications, the dark current reduces the dynamic range since the maximum signal is limited by the pixel charge integration capacitance, the last being partially filled with dark signal. The practical maximum acceptable requirements for dark current depend on the targeted SNR for the particular mission. Examples of mission-related parameters which influence the SNR are the spectral resolution, the spatial resolution, the operating temperature, the frame rate. The SNR depends also on the environmental properties like the spectral radiance at the detected wavelength and the total dose received during the mission for the related satellite orbit. Practical examples of how technical requirements are chosen for SWIR applications can be found in [16], [17].

The linearity relation between the dark current degradation and the fluence is valid at all the investigated bias. Therefore we can write:

$$\Delta J(V, \Phi) = \alpha(V) \times \Phi \tag{2}$$

where α is the Dark Current-related Damage Rate [18] and Φ the fluence. Figure 6 shows the coefficient α as a function of the reverse bias. The dependence of α on material properties

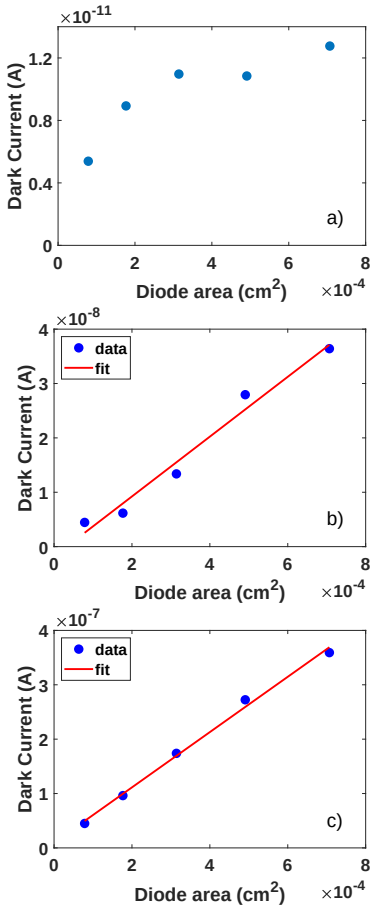

Fig. 4. Dark current at 5 V vs diode area a) before irradiation and at b) 2^{nd} fluence (3×10^{10} cm^{-2}), c) 4^{th} fluence (3×10^{11} cm^{-2}) for the five diodes of Table II.

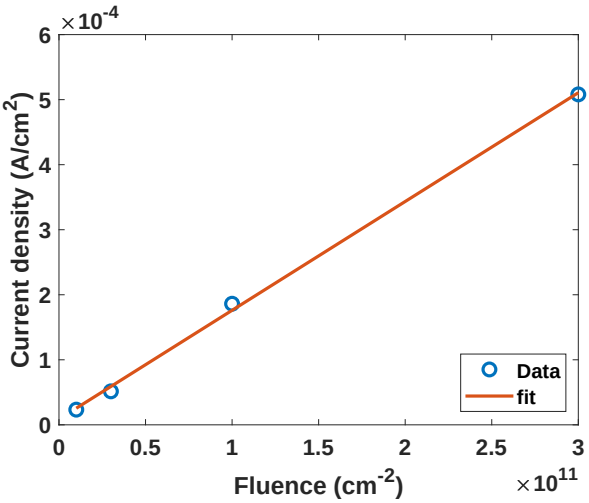

Fig. 5. Dark current density at 5 V as a function of the fluence for Diode5.

and measurement and irradiation conditions will be discussed in the case where the proton-induced current degradation is a generation current in the depletion region. These dependencies make a direct comparison with irradiation-induced degradation on SWIR HgCdTe detectors not directly applicable. Moreover, until now there have not been any public studies investigating

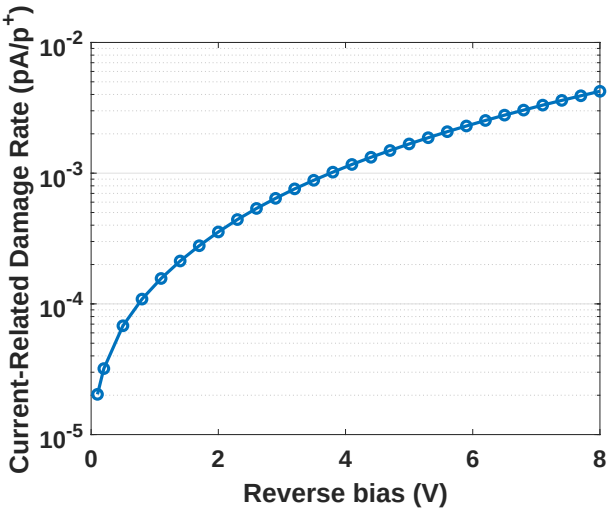

Fig. 6. Dark current-related damage rate for Diode5 as a function of the bias.

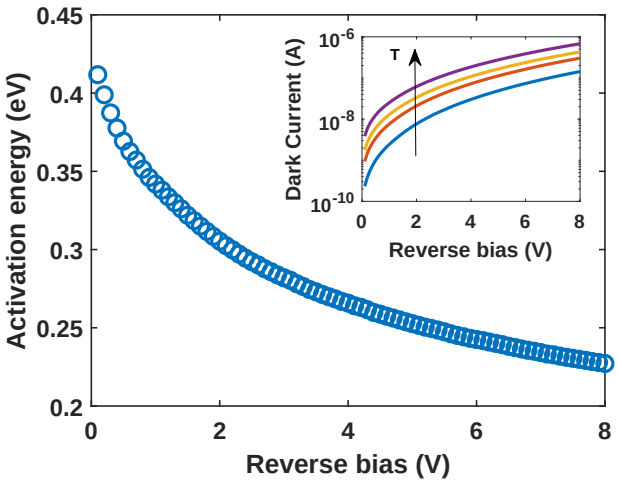

Fig. 7. Activation energy vs bias for Diode5. The activation energy was measured at the following temperatures: 250 K, 270 K, 280 K, and 293 K. The measurement has been performed 1 month after the 4th step. Inset: Dark Current vs Reverse bias at the four temperatures used for the calculation of the activation energy.

the irradiation effects on SWIR HgCdTe as absorbing material. An example of dark current degradation induced by proton irradiation on a complete NIR (Near-InfraRed) HgCdTe detector (detecting layer + ROIC) can be found in [19].

B. Activation energy

In order to understand the physical origin of the dark current after irradiation, it was important to understand its behavior in regard to temperature. In Fig. 7 the activation energy as a function of the reverse bias has been plotted for Diode5. All the five diodes showed the same behavior. The activation energy E_a has been computed from an Arrhenius law:

$$I = Ae^{-\frac{E_a}{kT}} \tag{3}$$

where the factor A is temperature independent. It is observed that the activation energy is much lower with respect to its value before irradiation (Fig. 3). Moreover, we note that the activation energy decreases when the reverse bias increases. At low reverse bias, the activation energy is about half the band gap energy of InGaAs (0.37 eV). This activation energy is typical for SRH generation current, whose temperature dependence follows the intrinsic carrier concentration n_i [20]. The decrease in activation energy with reverse bias is associated with field-enhancement mechanisms on the generation of carriers [12].

In order to investigate field enhancement effects, a proper model for the dark current is needed. This is the scope of the next section.

C. Field Enhancement Factor Extraction

Considering the employed fluences, $\Delta J(\Phi) = J_{post}(\Phi) - J_{pre} \approx J_{post}$ is a SRH generation current. The irradiation-induced SRH generation current density can be described by the integral of the electric field-dependent radiation-induced generation rate $\Delta U(F, \Phi)$ at fluence Φ over the depletion region width W:

$$\begin{aligned}\Delta J(V, \Phi) &= q \int_0^{W(V)} \Delta U(F(x, W), \Phi) \mathrm{d}x \\ &= q \Delta U_0(\Phi) \int_0^{W(V)} \Gamma^{GR}(F(x, W)) \mathrm{d}x\end{aligned} \tag{4}$$

where q is the elementary charge. The radiation-induced generation rate $\Delta U(F, \Phi)$ has been expressed in terms of the Generation Rate Field Enhancement Factor (GRFEF) Γ^{GR} as $\Delta U(F, \Phi) = \Delta U_0(\Phi) \times \Gamma^{GR}(F(x, W))$ where ΔU_0 is the radiation-induced generation rate per unit volume in absence of field effects. To justify this approach, we rewrite the typical generation rate through states within the bandgap [21] by introducing a field enhancement factor $\Gamma_{n(p)}$ [22] to the electron (hole) lifetime. The net radiation-induced generation rate can be written as:

$$\Delta U(F, \Phi) = \frac{n_i}{\tau_g(F, \Phi)} = n_i \left(\frac{\tau_n(\Phi)}{\Gamma_n(F)} + \frac{\tau_p(\Phi)}{\Gamma_p(F)} \right)^{-1} \tag{5}$$

where n_i is the intrinsic carrier concentration, τ_g the generation lifetime and $\tau_{n(p)}(\Phi)$ is the low field generation lifetime for electrons (holes) [23]:

$$\begin{cases} \tau_n(\Phi) = \tau_{n0} e^{-\frac{E_t - E_i}{kT}} \\ \tau_p(\Phi) = \tau_{p0} e^{\frac{E_t - E_i}{kT}} \end{cases} \tag{6}$$

We remark that the GRFEF Γ^{GR} expresses the enhancement of the electron-hole pair generation rate through states in the band gap and it should not be confused with $\Gamma_{n(p)}$, which expresses the field enhancement of the single transition rate between conduction (valence) band and the trap. Note also that we have dropped the symbol "Δ" in (5) because $\Delta J(\Phi) \approx J_{post}$. We can relate the two lifetimes as $\tau_{p0} = a \times \tau_{n0}$. The factor a depends on thermal velocity of carriers and the relative capture cross sections of electrons and holes [15]. Consequently:

$$\Delta U(F, \Phi) = \Delta U_0(\Phi) \Gamma^{GR}(F) \tag{7}$$

where

$$\begin{cases} \Delta U_0(\Phi) = \frac{n_i}{k\tau_{n0}(\Phi)} = \frac{n_i}{\tau_0(\Phi)} \\ \Gamma^{GR}(F) = k\left(\frac{e^{-\frac{E_t-E_i}{kT}}}{\Gamma_n(F)} + \frac{ae^{\frac{E_t-E_i}{kT}}}{\Gamma_p(F)}\right)^{-1} \end{cases} \quad (8)$$

$k = \Gamma^{GR^{-1}}(0)$ is a normalization constant such that $\Gamma^{GR}(0) = 1$. Its expression can be found by setting $\Gamma_{n(p)} = 1$. For example, for $E_t = E_i$ and $\tau_{n0} = \tau_{p0}$, then $k = 2$ and the formula reduces to the one found by [21]. The linear dependence of ΔJ with fluence (see (2)) suggests that the generation lifetime degradation is inversely proportional to the fluence, i.e. $\tau_0 \times \Phi = K_g$ where K_g is the generation lifetime damage factor. Therefore, we can rewrite (4) as:

$$\Delta J(V) = \left[q\frac{n_i}{K_g}\int_0^{W(V)} \Gamma^{GR}(F(x,W))\mathrm{d}x\right] \times \Phi \quad (9)$$

$\Delta U_0 = \frac{n_i}{K_g}\Phi$ can be assumed to be independent on position, assuming that SRH centers created by the proton irradiation are uniformly distributed in the InGaAs layer due to the large proton energy employed.

For a constant doping, it can be shown that:

$$\frac{\mathrm{d}(\Delta J)}{\mathrm{d}W} = q\Delta U_0 \Gamma^{GR}(F_{max}) \quad (10)$$

In the following, even if in our case the doping is not constant for the first 1 µm from the junction, we will consider that (10) applies. This can be justified by two arguments. The first is that the doping varies smoothly and the second is that the GRFEF is usually strongly dependent on the field.

In order to perform this analysis on experimental data, the depletion region width W has been extracted from $C-V$ measurements as $W(V) = \varepsilon\frac{1}{C_A(V)}$, where C_A is the capacitance density and ε is the dielectric constant of InGaAs. The capacitance density has been obtained from $C(V) = C_A(V) \times A + C_P(V)$ where C is the measured capacitance, A is the area of the diode, and C_P is the parasitic capacitance. To extract C_A, the three biggest diodes (Diode3,4,5) have been considered (Fig. 8). For all the doses, the capacitance at last dose has been used to extract W and perform the analysis. In fact, we have not observed important irradiation-induced changes in the capacitance with respect to the pre-iradiation values. The doping profile, which allows computing the maximum electric field at the junction, has been extracted for $x > W(0\text{ V})$ as $N(W) = \left[\frac{1}{2}q\varepsilon\frac{\mathrm{d}(C_A^{-2})}{\mathrm{d}V}\right]^{-1}$ as shown in Fig. 9. The doping profile at $x < W(0\text{ V})$ has been extrapolated from the $C(V)$ trend and modeled by a parabolic behavior. This may be due to donor compensation close to the junction. The maximum electric field range is $1.1-8.2\times10^6$ V/m in the reverse bias range $0-8$ V.

D. Damage Factor

The model shown in the previous section can be used to extract the Damage Factor K_{dark} in the case of presence of electric field effects. K_{dark} has been introduced by [8] to account for radiation-induced dark current in silicon devices. In particular, it properly describes the degradation when the dark current is dominated by thermal generation through bulk centers in the depletion region. K_{dark} is defined in [8] as the increase of thermal generation rate ΔU per unit of displacement damage dose D_d deposited:

$$K_{dark} = \frac{\Delta U}{D_d} \quad (11)$$

The displacement damage dose is defined as $D_d(E) = NIEL(E) \times \Phi$ where NIEL is the Non-Ionizing Energy Loss and E is the proton kinetic energy.

In the case of a uniform radiation-induced thermal generation rate ΔU over the depletion region W, the dark current increase has been expressed in [8] as:

$$\Delta J(V) = (q \times K_{dark} \times W(V) \times NIEL) \times \Phi \quad (12)$$

The only dependence of ΔJ in (12) on V is through W. However, this is the case where field enhancement mechanisms

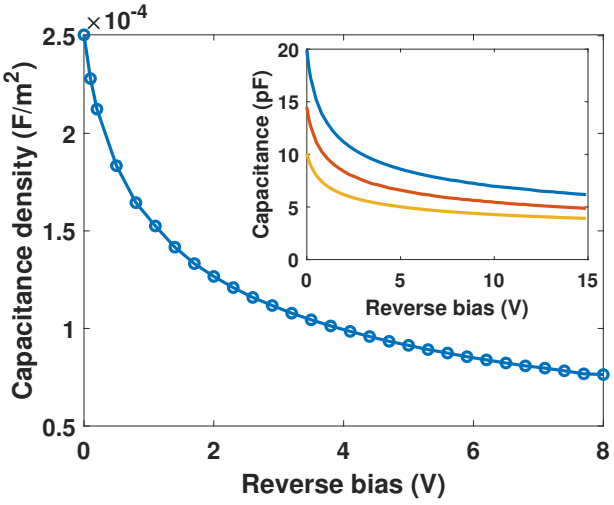

Fig. 8. Capacitance density measured one month after the 4^{th} fluence. Inset: Capacitance of the three biggest diodes from which the capacitance density is extracted.

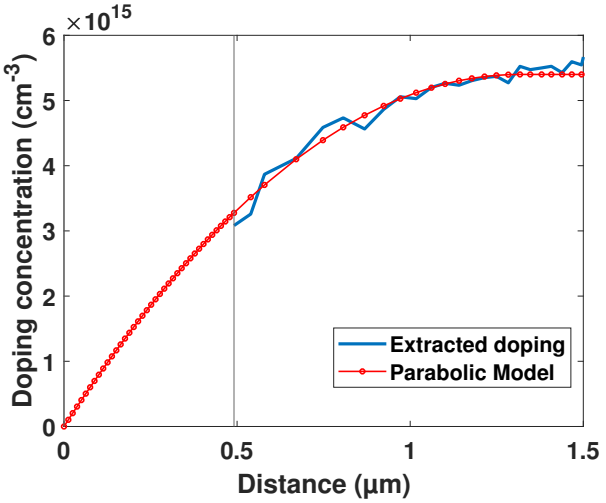

Fig. 9. Doping profile as a function of the depletion region width W. The red curve shows the profile used for the calculation, which is extrapolated from the $C(V)$-derived doping profile trend (in blue). The vertical dashed line is at $x = W(0\,\text{V})$.

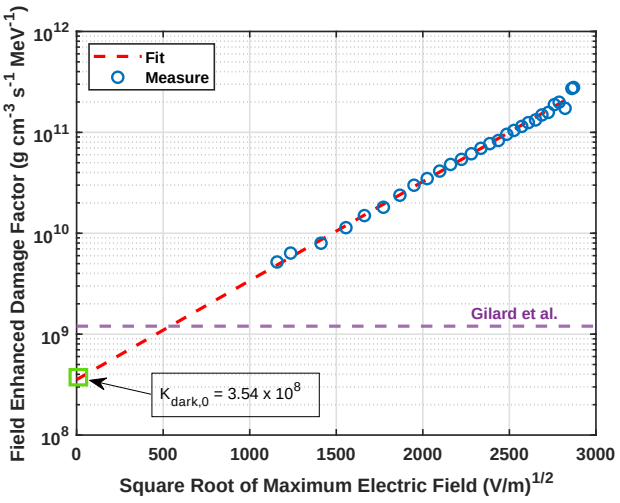

Fig. 10. Extraction of the low-field Damage Factor $K_{dark,0}$ at room temperature for Diode5 at the 4^{th} fluence (3×10^{11} cm^{-2}). In violet the value found by [4], independent on voltage.

are negligible ($\Gamma^{GR} = 1$). In our case, ΔJ being an electric field-enhanced generation current, it should be described by (9) rather than (12).

Relying on meta studies conducted on InGaAs photodiodes with similar structure [3], [4], which employed different proton energies and particles, we assume that the "NIEL scaling hypothesis" is valid in our case. This allow us to say that not only ΔJ is proportional to the fluence, but also to the NIEL as assumed by the model (12). In order to compare our damage factor with the one found by [4], [24] (where the authors used the model (12)), we rewrite (10) in terms of D_d as:

$$\frac{1}{qD_d}\frac{\mathrm{d}(\Delta J)}{\mathrm{d}W} = K_{dark,0}\Gamma^{GR}(F_{max}) \tag{13}$$

$K_{dark,0} = \frac{\Delta U_0}{D_d} = \frac{n_i}{K_g \times NIEL}$ is the dark current damage factor at low field and quantifies the generation rate degradation per unit of D_d deposited with no field enhancement effects. If $\Gamma^{GR} \approx 1$, then $K_{dark,0}$ corresponds to K_{dark} defined in [8] and used by [4], [24].

The experimental result of such analysis is shown in Fig. 10 for the Diode5 at the fourth dose. The GRFEF at room temperature turns out to follow the empirical law:

$$\Gamma^{GR}(F) = \exp\left(\sqrt{\frac{F}{F_0}}\right) \tag{14}$$

where $F_0 = 1.9 \times 10^5$ V/m. We note that the field enhancement ratio between 0 V and 8 V is about 40. All the diodes showed a similar trend at all the four fluences.

It is possible to extract $K_{dark,0}$ by looking at the intercept of $\log\left(\frac{1}{qD_d}\frac{\mathrm{d}\Delta J}{\mathrm{d}W}\right)$ vs $\sqrt{F_{max}}$ with the y-axis. The average value of the extracted damage factor (computed from all the fluences except the lowest, since at the lowest fluence the current proportionality with diode surface is less precise), considering Diode4 and Diode5, gives a value at ~ 293 K of $K_{dark,0} = 3.8 \times 10^8$ g $\cdot$ s^{-1} $\cdot$ MeV^{-1} $\cdot$ cm^{-3} using $NIEL = 3.6461 \times 10^{-7}$ MeV $\cdot$ m^2 $\cdot$ g^{-1} [25]. We remind that the extracted low field damage factor $K_{dark,0}$ is

TABLE III
LITERATURE COMPARISON OF DAMAGE FACTORS K_{dark} FOR INGAAS PHOTODIODES AT ROOM TEMPERATURE

	$\mathbf{K_{dark}(g \cdot s^{-1} \cdot MeV^{-1} \cdot cm^{-3})}$	**Comments**
This work	3.8×10^8	Low-field
[4]	1.2×10^9	Between 0 and 5 V
[24]	2.7×10^9	At 0.2 V

calculated from the $I_d - V$ measured on site right after each fluence. Since, we observed a room temperature annealing of about 20% of the dark current during the following month, K_{dark} follows the same trend. This annealing occurred in the first days after the irradiation; no further important annealing has been observed. This means that, when comparing K_{dark} with other references, attention should be paid at the time elapsed between the irradiation and the measurement. A comparison with the literature is shown in Table III. The main difference from the literature is expected to stem from the effect of the electric field that was not removed in [4], [24]. For example, [24] used the value of K_{dark} calculated at 0.2 V because they found a higher K_{dark} at higher reverse bias. They attributed this result to the onset of tunneling as field enhancement effect in the thermal generation. We highlight that the InGaAs doping concentration, in that study, was about one order of magnitude higher with respect to the present work.

We come back now to (14) in order to find a theoretical justification for such a result. We remind that the GRFEF depends on $\Gamma_{n(p)}$ as described in (8). There are mainly two electric field enhancement mechanisms for the generation of carriers through traps in the band gap: the Poole-Frenkel (PF) and the Phonon-Assisted Tunneling (PAT) [9]. In Fig. 11 the two mechanisms are represented in the case of an electron emission from a Coulombic well in the presence of a constant electric field F. The electric field is considered constant, giving a contribution to the potential $-qFr$ (local field approximation). The same picture applies for hole emission, where the barrier seen by holes where no electric field is present is $E_g - E_t$, E_g being the band gap energy. Vincent et al. [9] gave an analytical expression for the one-dimensional (1-D) field enhancement factors associated to these mechanisms in the case of a trap with a Coulombic potential. After defining $z = \frac{E}{kT}$, we have:

$$\Gamma(F)_{PF} = \exp\left(\frac{\Delta E(F)}{kT}\right) \tag{15a}$$

$$\Gamma(F)_{PAT} = \int_{\frac{\Delta E}{kT}}^{\frac{E_t}{kT}} \exp\left(z - z^{3/2} f(F) g(F)\right) \mathrm{d}z \tag{15b}$$

where

$$\begin{cases} f(F) = \left[\frac{4}{3}\frac{(2m^*)^{1/2}(kT)^{3/2}}{q\hbar F}\right] \\ g(F) = \left(1 - \left(\frac{\Delta E(F)}{zkT}\right)^{5/3}\right) \end{cases}$$

and the barrier lowering is $\Delta E(F) = \left(\frac{q^3 F}{\pi\varepsilon}\right)^{1/2}$.

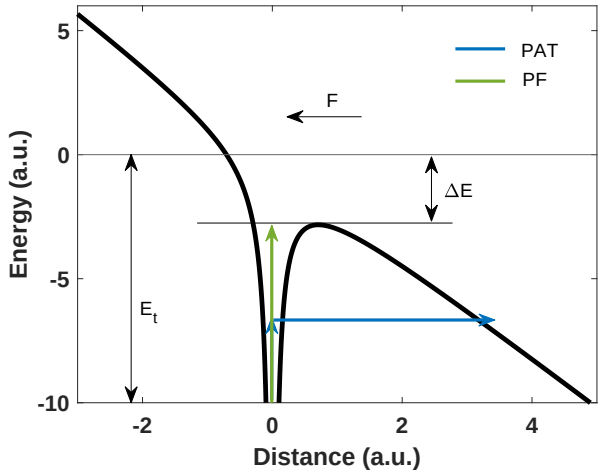

Fig. 11. Poole-Frenkel and Phonon-Assisted Tunneling electron emission enhancement for a Coulombic well. In the figure, the trap is located at $r = 0$ and $E = 0$ represents the energy at which the electron would be free in the absence of the electric field F. E_t is the energy of the trap measured from the conduction band edge and ΔE_n is the barrier lowering see by an emitted electron due to the local field F.

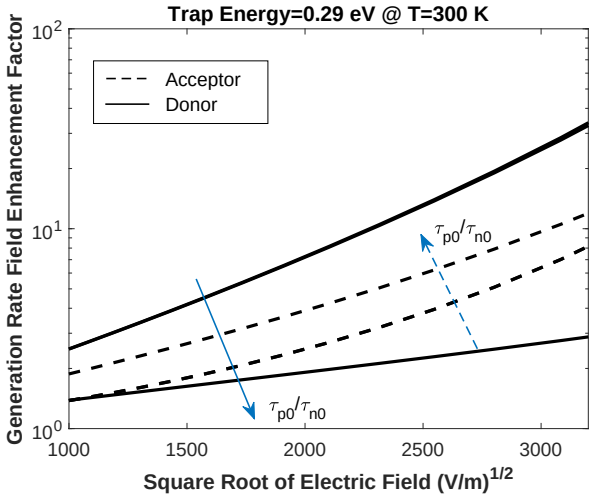

Fig. 12. Simulated Generation Rate Field Enhancement Factor at 300 K as a function of the square root of the electric field with a as parameter for an acceptor trap (dashed line) and a donor trap (solid line). The solid arrow points towards the higher a for the donor trap whereas the dashed arrow points towards the higher a for the acceptor trap. The used tunneling effective masses are $m_n = 0.034m_0$ and $m_p = 0.46m_0$ [27].

At first glance, our experimental GRFEF Γ^{GR} has a field dependence similar to the PF. A similar law for the GRFEF was found by [11] who studied the generation current in silicon $\mathrm{n}^+ - \mathrm{p}$ junctions. In [11], they found however a value for F_0 lower than expected. Similarly, our extracted F_0 is about 10 times lower than the expected one for InGaAs $F_0 = \left(\frac{q^3}{\pi\varepsilon k^2 T^2}\right)^{-1} = 1.56 \times 10^6$ V/m at 293 K.

We have tried to explain this inconsistency by simulating the GRFEF. Coming back to (8), the GRFEF is defined as:

$$\Gamma^{GR}(F) = k\left(\frac{e^{-\frac{E_t - E_i}{kT}}}{\Gamma_n(F)} + \frac{ae^{\frac{E_t - E_i}{kT}}}{\Gamma_p(F)}\right)^{-1} \tag{16}$$

where $\Gamma_{n(p)}(F) = \Gamma_{PAT,n(p)}(F) + \Gamma_{PF}(F)$ is the electron (hole) emission enhancement factor.

In order to explain our empirical GRFEF by means of PF and PAT mechanisms, we have plotted in Fig. 12 the simulated GRFEF of (16) in the case of a trap with energy $E_t = 0.29$ eV from the conduction band edge for different values of $a = \frac{\tau_{p0}}{\tau_{n0}}$. This trap energy has been found by Shaw et al. [26] to be responsible for the generation of current in electron-irradiated InGaAs photodiodes. However, other literature studies are not in accordance on this value. Nelson et al. [24] found $E_t = 0.44$ eV for proton-irradiated InGaAs photodiodes.

Although we tried to tune the model parameters, we have not been able to explain a Γ^{GR} ratio of about 40 between electric field values of 10^6 and 10^7 V/m. We are inclined to believe that a PAT-limited GRFEF is the only possibility because the PF effect has a much weaker field dependence than the one we have found in our experimental GRFEF [9]. One possibility could be that in our case PAT is induced in defect clusters where very high local fields [5] can be present. This charged clusters are of the order of the Debye length $L_D = \sqrt{\frac{\epsilon kT}{q^2 N_D}} \approx 60\,\mathrm{nm}$ as can be shown by Monte Carlo simulations [18] and therefore they are not detected by $C - V$

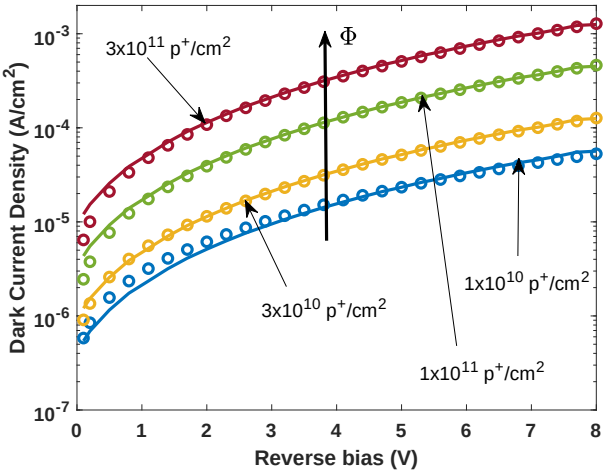

Fig. 13. Dark current density as a function of the reverse bias at each dose for Diode 5. The circled curves represent the measurement whereas the solid curves show the simulation using (4) where the experimental GRFEF obtained from the model described by (10) has been used for all the fluences. The low-field generation lifetime τ_0, defined in (8), is the fitting parameter.

measurements. Given the difficulties to find a match between models and experience, we keep this analysis quite empirical.

To double check that (14) really does describe the voltage dependence (and consequently the field dependence) of the dark current after irradiation at room temperature, this model has been used to compute the dark current as in (4). There is a good match between the model and the measurement, as shown in Fig. 13. The fitted generation lifetimes τ_0 are indicated in Table IV. Figure 14 shows the generation lifetime degradation with fluence. A generation lifetime damage factor $K_g = 1.12 \times 10^{10}$ $\mathrm{p}^+ \cdot \mathrm{s} \cdot \mathrm{m}^{-2}$ has been found. We remind that this lifetime is defined by (8) and it should not be confused with the recombination lifetime extracted from time-

TABLE IV
EXTRACTED LOW-FIELD GENERATION LIFETIME AS A FUNCTION OF FLUENCE

Fluence (cm^{-2})	**Generation Lifetime (µs)**
1×10^{10}	91
3×10^{10}	36
1×10^{11}	11
3×10^{11}	3.71

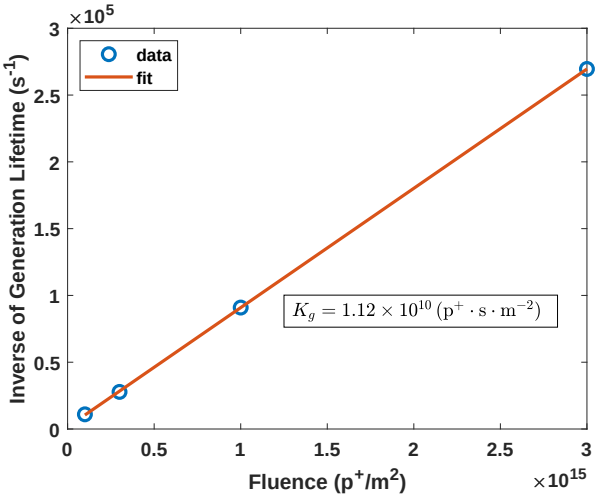

Fig. 14. Inverse of the low-field generation lifetime τ_0 as a function of the fluence.

resolved photoluminescence (TR-PL) measurements. In fact, the recombination lifetime in TR-PL experiments is extracted in the low-injection conditions and it is given by:

$$\tau_r^{-1} = \tau_{rad}^{-1} + \tau_{SRH}^{-1} + \tau_{Aug}^{-1} \tag{17}$$

In the case of n-doped semiconductor, τ_{rad} is the radiative recombination lifetime, $\tau_{SRH} = \tau_{p0}$ and τ_{Aug} is the Auger recombination lifetime. Expressions for τ_{rad} and τ_{Aug} can be found in [28].

IV. CONCLUSION

The degradation of InGaAs PIN photodiodes due to 49.7 MeV proton irradiation at 293 K has been studied. The sample availability at the III-V Lab allowed us to study the InGaAs photodiode degradation, without the influence of any Read Out Integrated Circuit, the last being the case in [1], [2], [5], [6]. The dark current degradation turns out to be proportional to the fluence and it is due to the creation of SRH generation centers in the depletion region of InGaAs. A model based on the SRH generation current has been developed to consider the role of the electric field on the enhancement of the thermal carrier generation. An experimental Generation Rate Field Enhancement Factor has been extracted. Its dependence on the electric field has been addressed starting from the fundamental physics of field-assisted emission of a carrier from a potential trap. The match between the theoretical calculations that we conducted and the experiments was not straightforward because the theoretical models include several parameters to which we did not have access. Because of the strong dependence of the GRFEF on the field, we suspect that tunneling is the main mechanism. The GRFEF has been included in the definition of the Damage Factor. A low-field damage factor has been extracted and compared to other studies of proton irradiation on InGaAs photodiodes. As expected, removing the effects of the electric field lowers its value. This suggests the use, in space applications, of a reverse bias as low as reasonably possible in order to reduce electric field enhancement effects. Moreover, the doping concentration should be also reduced. As the final result of our analysis, the low-field generation lifetime degradation has been extracted. Its value is dependent on the position of the trap level in the band gap. Further DLTS data could help in having a more complete understanding of the trap energy level responsible for the degradation.

ACKNOWLEDGMENT

The authors gratefully acknowledge CNES and Thales Alenia Space for co-funding this research. They have also appreciated valuable discussions with B. Vinter.

REFERENCES

[1] X. Hugon, O. Amore, S. Cortial, C. Lenoble, and M. Villard, "Near-room operating temperature SWIR InGaAs detectors in progress," in *Infrared Technology XXI* (B. F. Andresen and M. Strojnik, eds.), vol. 2552, pp. 738 – 747, International Society for Optics and Photonics, SPIE, September 1995.

[2] L. Tauziede, K. Beulé, M. Boutillier, F. Bernard, J.-L. Reverchon, and A. Buffaz, "Evaluation of InGaAs array detector suitability to space environment," in *International Conference on Space Optics — ICSO 2012* (B. Cugny, E. Armandillo, and N. Karafolas, eds.), vol. 10564, p. 105640O, International Society for Optics and Photonics, SPIE, 2017.

[3] T. Nuns, C. Inguimbert, J. Barbero, J. Moreno, S. Ducret, A. Nedelcu, B. Galnander, and E. Passoth, "Displacement damage effects in InGaAs photodiodes due to electron, proton, and neutron irradiations," *IEEE Transactions on Nuclear Science*, vol. 67, pp. 1263–1272, July 2020.

[4] O. Gilard, L. S. How, A. Delbergue, C. Inguimbert, T. Nuns, J. Barbero, J. Moreno, L. Bouet, S. Mariojouls, and M. Boutillier, "Damage factor for radiation-induced dark current in InGaAs photodiodes," *IEEE Transactions on Nuclear Science*, vol. 65, pp. 884–895, March 2018.

[5] S. Barde, R. Ecoffet, J. Costeraste, A. Meygret, and X. Hugon, "Displacement damage effects in InGaAs detectors: experimental results and semi-empirical model prediction," *IEEE Transactions on Nuclear Science*, vol. 47, pp. 2466–2472, December 2000.

[6] Q. Kleipool, R. Jongma, A. Gloudemans, H. Schrijver, G. Lichtenberg, R. van Hees, A. Maurellis, and R. Hoogeveen, "In-flight proton-induced radiation damage to SCIAMACHY's extended-wavelength InGaAs near-infrared detectors," *Infrared Physics & Technology*, vol. 50, pp. 30–37, March 2007.

[7] C. Leroy and P.-G. Rancoita, *Principles of Radiation Interaction in Matter and Detection*. WORLD SCIENTIFIC, 4th ed., 2016.

[8] J. Srour and D. Lo, "Universal damage factor for radiation-induced dark current in silicon devices," *IEEE Transactions on Nuclear Science*, vol. 47, pp. 2451–2459, December 2000.

[9] G. Vincent, A. Chantre, and D. Bois, "Electric field effect on the thermal emission of traps in semiconductor junctions," *Journal of Applied Physics*, vol. 50, no. 8, pp. 5484–5487, 1979. Published Online: 29 July 2008.

[10] Y. Murakami and T. Shingyouji, "Separation and analysis of diffusion and generation components of pn junction leakage current in various silicon wafers," *Journal of Applied Physics*, vol. 75, no. 7, pp. 3548–3552, 1994. Published Online: 04 June 1998.

[11] A. Poyai, E. Simoen, and C. Claeys, "Impact of a high electric field on the extraction of the generation lifetime from the reverse generation current component of shallow n^+p-well diodes," *IEEE Transactions on Electron Devices*, vol. 48, pp. 2445–2446, October 2001.

[12] E. Simoen, F. De Stefano, G. Eneman, B. De Jaeger, C. Claeys, and F. Crupi, "On the temperature and field dependence of trap-assisted tunneling current in Ge p^+n junctions," *IEEE Electron Device Letters*, vol. 30, pp. 562–564, May 2009.

[13] A. Rouvié, J.-L. Reverchon, O. Huet, A. Djedidi, J.-A. Robo, J.-P. Truffer, T. Bria, M. Pires, J. Decobert, and E. Costard, "InGaAs focal plane array developments at III-V Lab," in *Infrared Technology and Applications XXXVIII* (B. F. Andresen, G. F. Fulop, and P. R. Norton, eds.), vol. 8353, p. 835308, International Society for Optics and Photonics, SPIE, 2012.

[14] A. Djedidi, A. Rouvie, J. Reverchon, M. Pires, N. Chevalier, and D. Mariolle, "Investigation of the influence of Zn-diffusion profile on the electrical properties of InGaAs/InP photodiodes," in *2012 International Conference on Indium Phosphide and Related Materials*, pp. 110–112, 2012.

[15] S. M. Sze, K. K. Ng, and Y. Li, *Physics of semiconductor devices*. Wiley, fourth edition ed., 2021.

[16] A. Dariel, P. Chorier, C. Leroy, A. Maltère, V. Bourrillon, B. Terrier, M. Molina, and F. Martino, "Development of an SWIR multispectral detector for GMES/Sentinel-2," in *Sensors, Systems, and Next-Generation Satellites XIII* (R. Meynart, S. P. Neeck, and H. Shimoda, eds.), vol. 7474, p. 747416, International Society for Optics and Photonics, SPIE, 2009.

[17] B. Sierk, J.-L. Bézy, A. Löscher, and Y. Meijer, "The European CO2 Monitoring Mission: observing anthropogenic greenhouse gas emissions from space," in *International Conference on Space Optics — ICSO 2018* (Z. Sodnik, N. Karafolas, and B. Cugny, eds.), vol. 11180, p. 111800M, International Society for Optics and Photonics, SPIE, 2019.

[18] M. Moll, *Radiation damage in silicon particle detectors: Microscopic defects and macroscopic properties*. PhD thesis, Hamburg U., 1999.

[19] P.-E. Crouzet, S. Tetaud, D. Gooding, B. Shortt, T. Beaufort, S. Blommaert, B. Butler, G. V. Duinkerken, J. ter Haar, F. Lemmel, K. van der Luijt, and H. Smit, "First proton and gamma radiation of the MCT NIR European astronomy large format array detector," in *X-Ray, Optical, and Infrared Detectors for Astronomy IX* (A. D. Holland and J. Beletic, eds.), vol. 11454, p. 114542N, International Society for Optics and Photonics, SPIE, 2020.

[20] S. R. Forrest, R. F. Leheny, R. E. Nahory, and M. A. Pollack, "In0.53Ga0.47As photodiodes with dark current limited by generation-recombination and tunneling," *Applied Physics Letters*, vol. 37, no. 3, pp. 322–325, 1980. Published Online: 22 July 2008.

[21] C.-t. Sah, R. N. Noyce, and W. Shockley, "Carrier generation and recombination in p-n junctions and p-n junction characteristics," *Proceedings of the IRE*, vol. 45, pp. 1228–1243, September 1957.

[22] G. Hurkx, D. Klaassen, and M. Knuvers, "A new recombination model for device simulation including tunneling," *IEEE Transactions on Electron Devices*, vol. 39, pp. 331–338, February 1992.

[23] D. Schroder, "The concept of generation and recombination lifetimes in semiconductors," *IEEE Transactions on Electron Devices*, vol. 29, pp. 1336–1338, August 1982.

[24] G. T. Nelson, G. Ouin, S. J. Polly, K. B. Wynne, A. W. Haberl, W. A. Lanford, R. A. Lowell, and S. M. Hubbard, "In situ deep-level transient spectroscopy and dark current measurements of proton-irradiated InGaAs photodiodes," *IEEE Transactions on Nuclear Science*, vol. 67, pp. 2051–2061, September 2020.

[25] [Online]. Available: https://www.sr-niel.org/.

[26] G. J. Shaw, S. R. Messenger, R. J. Walters, and G. P. Summers, "Radiation-induced reverse dark currents in In0.53Ga0.47As photodiodes," *Journal of Applied Physics*, vol. 73, pp. 7244–7249, June 1993.

[27] A. W. Walker and M. W. Denhoff, "Heavy and light hole minority carrier transport properties in low-doped n-InGaAs lattice matched to InP," *Applied Physics Letters*, vol. 111, p. 162107, October 2017.

[28] E. Rosencher and B. Vinter, *Optoelectronics*. Cambridge University Press, 2002.